CNG direct injection spark-ignition engine with high turbulence and high compression ratio: numerical and experimental investigations

Loic Rouleau, David Serrano, Bertrand Lecointe, Frédéric Ravet, Gilles Coma, Panos Christou

CNG direct injection spark-ignition engine with high turbulence and high compression ratio: numerical and experimental investigations

Loïc Rouleau, David Serrano, Bertrand Lecointe

Powertrain and Vehicle Division
IFP Energies nouvelles, Institut Carnot IFPEN Transports Energie
Rond-point de l'échangeur de Solaize, BP 3, 69360 Solaize, France
loic.rouleau@ifpen.fr, david.serrano@ifpen.fr, bertrand.lecointe@ifpen.fr

Frédéric Ravet, Gilles Coma, Panos Christou

DEA-IR, Thermal engine innovation
Renault, Technocentre
1 avenue du Golf – 78084 Guyancourt, France, frederic.ravet@renault.com,
gilles.coma@renault.com, panagiotis.christou@renault.com

Abstract: This study carried on within the H2020 GasOn project scope of work showed the interest to improve the turbulence of a CNG direct injection spark ignited engine with high compression by a dedicated cylinder head design. The in-cylinder air motion was optimally configured through 3D-CFD simulation in order to cope with the high performance targets (~240 N.m/L at 1500 rpm, ~80kW/L at 4500 rpm) within the cylinder pressure limit of 160 bar ($P_{cylmax}+2\sigma$ = 180 bar). To sustain such level of pressure a Diesel engine basis was used. The compression ratio was set to 13.4:1 in line with the knock resistance of the natural gas. This newly design engine was compared to a reference engine developed in a previous study. The flow test bench measurements confirmed the high tumble level of the optimized cylinder head. This new cylinder head was next tested on a single cylinder engine equipped with high mass flow rate gas injector prototype developed by Continental. The results, integrating the boundary conditions of the air path system including LP-EGR, validated the good effect of faster combustion revealed by the lower fuel consumption and the high tolerance to EGR dilution in stoichiometric conditions. Consequently, the results showed a significant improvement compared to the previous engine and a performance attaining Diesel-like break thermal engine efficiencies (~41%).

1 Objectives and motivations

The evolution of European regulation applied to internal combustion engines (ICE) becomes more and more stringent particularly about pollutants emissions[1].

Compressed natural gas (CNG) appears as one of the most promising alternative fuel solution since it is available worldwide and has some good intrinsic properties for internal combustion engine applications[2]. CNG is mostly composed of methane which contains less carbon than other fossil fuels, such as gasoline or Diesel, that makes the balance between CO_2 emission and energy positive. Besides, CNG does not contain any aromatic compounds or any other soot precursors so the risk of particulate emissions coming from its combustion is nearly inexistent. Finally, CNG has a high knock resistance, since the estimated RON index of methane is close to 130. This low knock sensitivity allows using a higher compression ratio (13:1 to 14:1) than usually adopted on spark ignition (SI) engine (9:1 to 12:1). This is a good path to higher thermal efficiency. In this case, efficiency is not sufficient without achieving specific performance similar to a Diesel engine, and mainly the specific low end torque value. High combustion velocity is thus required and appropriate boosting solution will have to be adapted on purpose.

Today bi-fuel engine does not exploit all the advantages of CNG fuel properties. The purpose of this study within the H2020 GasOn European project scope of work was to design a high efficient SI engine using a direct injection (DI) of gas and dedicated to passenger cars (PC) or light duty vehicles (LD). In order to achieve such high specific performance, the engine will require a high compression ratio, a high boosting system associated to high turbulence combustion system. Such characteristics will lead to very high in-cylinder pressure and consequently to high mechanical constraints. The engine will have to sustain such levels of pressure and forces, this is why it was decided to use a Diesel based engine that fit with such requirements.

CNG is usually injected into the intake manifold, leading to a decrease in power output due to a lower volumetric efficiency. Using a direct injection system allows introducing separately air and gas into the combustion chamber. Moreover, the direct injection timing should be optimized as it has a strong impact on the mixing process (local air fuel ratio AFR), the turbulence level, the volumetric efficiency and the intake pressure required.

It is assumed that late injection reduces mixing time and favours an heterogeneous air/fuel mixture. But the required boost pressure is reduced due to an efficient air filling. This allows potentially to reach higher performance by exploiting this remaining margin in boost pressure. In the specific case of very late injection, during the second half of the compression stroke, the CNG plume can add a positive contribution to the turbulence generated during the intake stroke[3]. This case is out of scope in our study since we implemented a low pressure DI system up to 20bar (EOI below 64 CAD BTDC).

On the other hand, in case of early injection, the mixing time is longer and the CNG plume does not affect the turbulence generated during the intake stroke. This allows to improve the mixing process and enhance the combustion rate. But, in these conditions, the boost pressure needs to be higher than in late injection due to lower volumetric efficiency.

The optimal trade-off should be found between all these parameters and this aspect will be highlighted by the presented results and discussed in the experimental phase.

SI downsized engines commonly use scavenging process to improve the boosting process and postpone the knock limit[4]. However, this technology have been limited by HC emissions coming from the fuel short-circuiting the combustion chamber during the positive valve overlap. DI has thus been used on purpose on gasoline engine to limit or cancel this phenomenon by using appropriate injection timing strategies. Up to now, no DI gas device was available on the market to enhance gas engine behaviour towards high efficiency. This study proposes to assess the benefit brought by a new DI gas system developed by Continental with the support of the EU within the GasOn project. Besides, DI can also be needed to insure a catalyst heating[5] for low load and engine speed by an injection after the combustion.

Stoichiometric combustion was chosen in opposition to lean combustion to insure an efficient conversion of the pollutant emissions using a three way catalyst (TWC) with higher active noble metal content required by the higher methane stability compared to gasoline. This aftertreatment system remained at affordable cost in comparison with lean DeNOx aftertreatment.

EGR is currently used in most of the recent SI engines in stoichiometric combustion to gain in output power or indicated efficiency by allowing to stretch the knock limit at high load and high engine speed and also to control the exhaust temperature. Besides, dilution brought by EGR permits to improve indicated efficiency at low load due to the de-throttling effect leading to a reduced pumping work and heat transfer losses. Finally, EGR at stoichiometry is compatible with the conventional TWC which is cost effective compared for example to the aftertreatment system required for lean burn dilution. But EGR affects the combustion rate which is already low for CNG compared to gasoline. The combustion rate needs to be enhanced with EGR and this aspect will be emphasized in the present study.

The main work of this study was to develop a high efficient lambda one SI gas engine to be implemented on a PC or LD vehicle family. This work was carried out within the H2020 Gason project. The cylinder head was designed for a propagation flame combustion type using a pent roof profile. 3D-CFD RANS simulation was used to improve the turbulence and turbulent kinetic energy to fasten the combustion compared to a previous engine developed within the bilateral Mogador project[6] between Renault and IFPEN. These previous program results will be used as a reference, and will be entitled “previous engine”.

It is assumed that CNG combustion involves two main challenges: mixing CNG with fresh air and accelerate the intrinsic slow CNG combustion[7]. The mixing process is driven by the tumble motion generated by the air passing through the intake duct. However, appropriate mixing is not sufficient for efficient combustion. Indeed, a high turbulent kinetic energy is also required in the combustion chamber just before spark occurs to counterbalance the low laminar burning velocity of CNG and to achieve the targeted high performance. This high level of kinetic energy is achieved by an adequate design of both intake ducts and combustion chamber. The shape of intake ducts creates a high tumble motion during the intake stroke that is converted into local turbulent kinetic energy at the end of the compression stroke when reaching the top dead centre (TDC). The design of the combustion chamber helps to maintain a high residual turbulent kinetic energy through the compression stroke until spark ignition occurs. Spark plug and injector locations are also important to favour respectively the ignition and turbulence.

The cylinder head were therefore designed taking into account these needs leading to high indicated efficiency as well as a higher tolerance to EGR. This numerical investigation was based on the Mogador design[6] with pent roof shape, 4 valves, central CNG-DI injector, central spark plug and piston with a central shallow bowl. The final GasOn solution was achieved by the optimization of the intake duct and valve shape, injector or spark plug orientation and protrusion. This cylinder head was then manufactured and validated on flow test bench.

The optimized cylinder head was finally tested using a Single Cylinder Engine (SCE) based on CNG-DI spark ignition engine with high compression ratio. New CNG-DI injector prototype developed by Continental was implemented on the engine and delivers a high mass flow rate (12 g/s) at moderate pressure (20 bar) to achieve a high output power[8] and a high vehicle autonomy. This experimental study included the optimized injection timing, the global engine behaviour, the tolerance to LP-EGR. The results were compared to the experimental data achieved on the Mogador project[6].

2 Designing study

2.1 Background

A study, similar to the Mogador project[6], was done to design a high efficient CNG direct injection spark ignited engine. The in-cylinder air motion was optimally configured through 3D-CFD simulation in order to cope with the high performance targets within the cylinder pressure limit of 160 bar ($Pcylmax+2\sigma$ = 180 bar). To sustain such level of pressure a Diesel engine basis was used. The concept consisted in keeping the same based engine but changing the combustion head to switch from in-cylinder swirl motion to tumble motion more adapted to spark ignition engine. The compression ratio was also decreased to fit with a SI combustion type but was maintained fairly high (13.4:1) to take advantage to the high knock resistance of the CNG. Basic dimensions of both Mogador and GasOn engines are very close and gathered in Table 1.

Table 1: Comparison between previous and new engine characteristics

	Previous engine (Mogador)[6]	New engine (GasOn)
Displacement (cm^3)	365	402
Bore (mm)	76	80
Stroke (mm)	80.5	80
Number of valves	4	4
Compression ratio	13.2	13.4

2.2 Design methodology

The objective of this design phase process was to determine the shape of the intake duct to respect the compromise between air filling needed to meet the target of performance and the level of tumble to insure an efficient combustion.

The air filling capability was determined at maximum power condition and calculated at maximum torque conditions. The tumble level was optimized only at maximum torque conditions.

The design process is shown on Figure 1. The air filling optimization process addresses valves dimensions, valves diameters, valve lift profiles and global air loop architecture. The optimisation of trade-off between Tumble level and permeability was achieved through appropriate intake duct shape design.

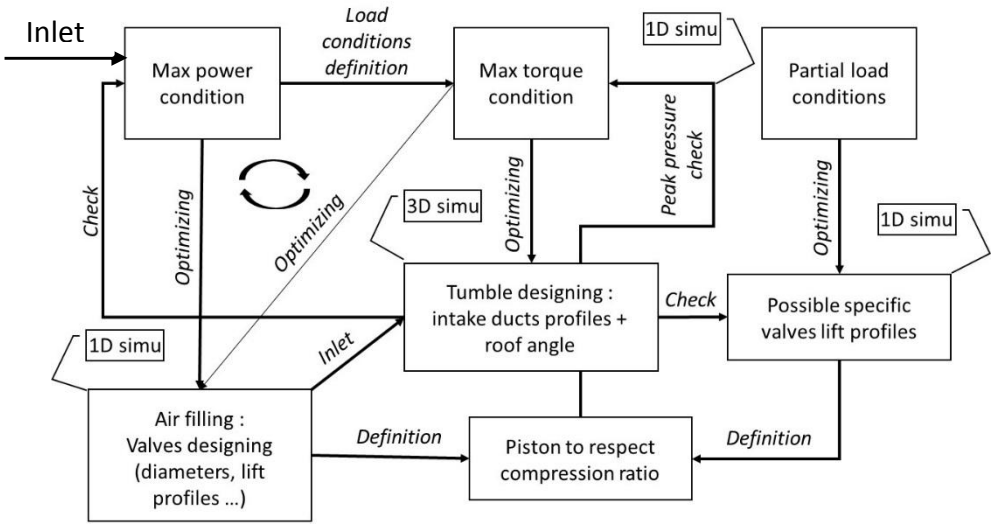

Figure 1: Design process

2.3 3D CFD set-up

3D simulations was used to optimize the design of the inlet ducts and obtain values to describe the air motion and the flame characteristics in order to evaluate the tested configurations with the Borghi - Peters diagram (see the next paragraph).

3D simulations were completed with CONVERGE code[9] which is a cut-cells code using auto-mesh technique and automatic mesh refinement algorithm. Thus, delays from geometries to simulation results are very short, lower than 10 hours.

Since inlet and outlet pressure conditions are applied, a numerical plenum was added to avoid any reflected numerical pressure waves from the boundary conditions (Figure 2).

k-Epsilon Reynolds Navier-Stokes (k-ε RNG) turbulence model was applied[10] in basic formulation.

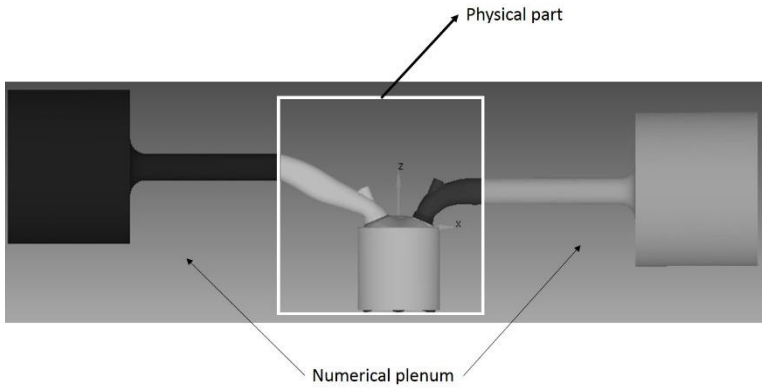

Figure 2: Numerical set-up of the simulation

2.4 Bridge between tumble and efficient combustion: Borghi - Peters diagram

Tumble motion is a number usually applied to characterize internal aerodynamic of the engine but the number is not sufficient enough to determine whether the internal aerodynamic level is adequate to achieve a high combustion efficiency.

We characterize the internal aerodynamic by using regime combustion diagram of Borghi-Peters[11]. The Borghi - Peters diagram (Figure 3) describes the different structures of a turbulent premixed flame front. In horizontal line, the ratio of the turbulent integral scale and the laminar flame thickness addresses the level of wrinkle of the flame front (wrinkle ratio). In vertical line, the ratio of the turbulent velocity and the laminar flame velocity addresses the level of stretch of the flame front (stretch ratio).

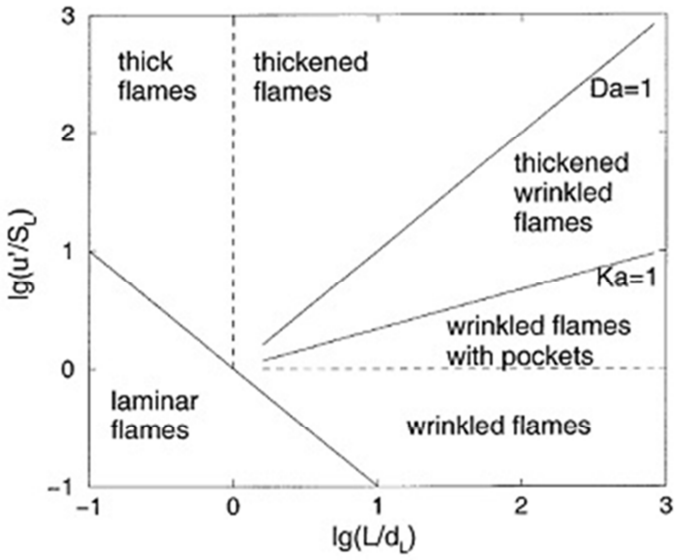

Figure 3: Borghi - Peters diagram

In automotive industry, high efficient combustion is limited by the boundary Karlovitz number (Ka) equal to 1. The higher the wrinkle level is, the faster is the turbulent flame front and the higher is the corresponding combustion efficiency. By the meantime, the stretch level[12] is limited by the combustion instabilities.

We designed the intake ducts using 3D-CFD simulation in fast loop design process to determine the location of each technical solution in the Borghi – Peters diagram. Each configuration was compared to the previous engine concept[6] considered as the reference and the objectives were to improve both the wrinkle and the stretch rates within the limit defined previously (Figure 4).

Finally, the configuration with the most significant improvement, respecting the air filling conditions determined to meet target of torque was selected. The deviation on the expected air filling for the selected configuration was lower than 0.2%.

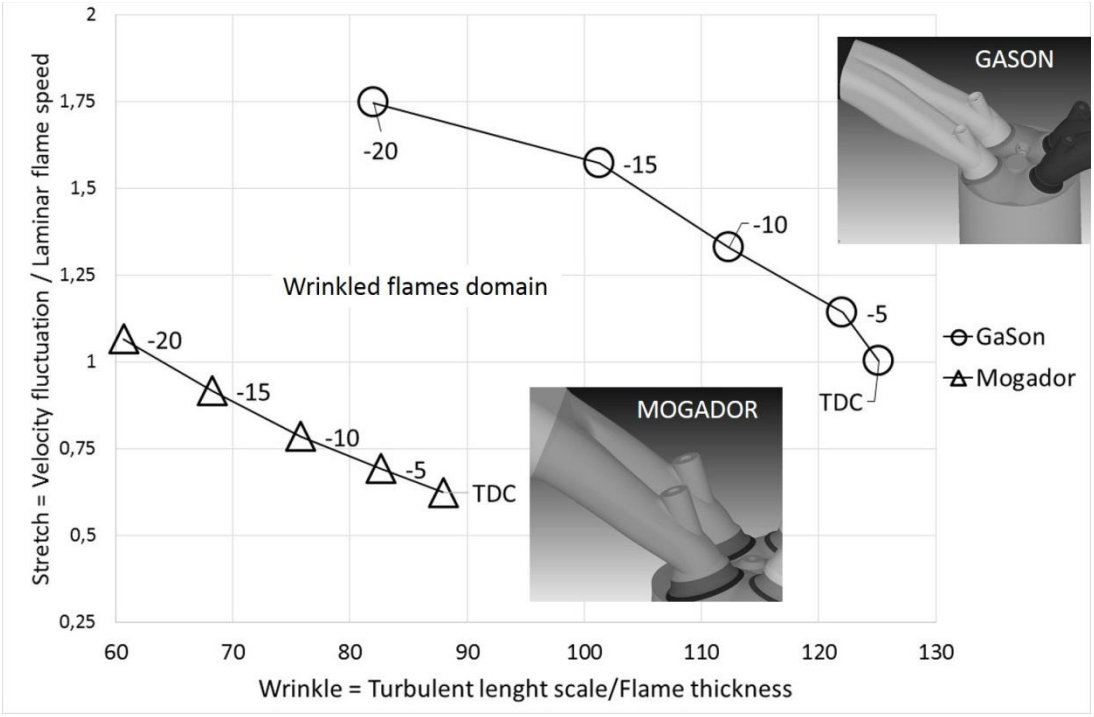

Figure 4: Manifolds of GasOn concept and Mogador concept versus crank angle at maximum torque condition in Borghi – Peters diagram

2.5 Flow check

Both GasOn concept and Mogador concept were characterized in a dedicated flow bench after manufacturing. Tumble and permeability coefficients were specific to the applied measurement method (Renault method) and only comparison between the two concepts could be done. The balance between tumble and permeability determined on Mogador concept was moved towards higher tumble and lower permeability on GasOn concept, corresponding to the expectations (Figure 5).

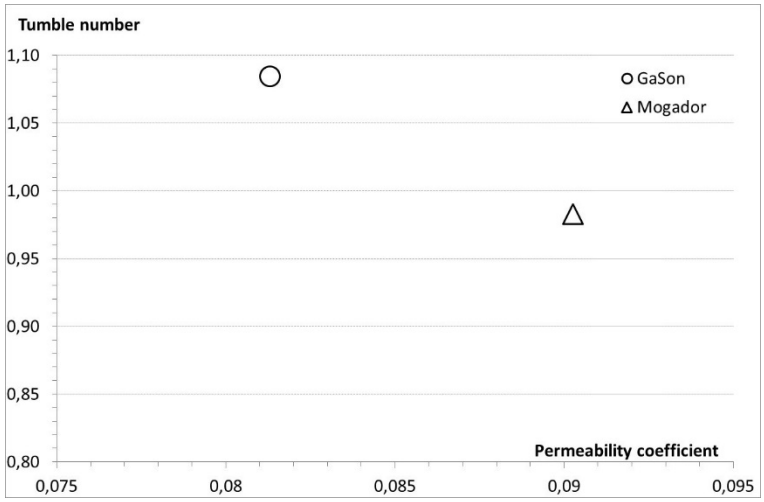

Figure 5: Flow bench results for GasOn concept and Mogador concept

2.6 Homogeneity index check

A specific set-up was implemented for the CNG injection system modelling. The concept of the CNG injection system was a valve of 7.4 mm diameter. The CNG valve lift profile was provided by Continental which developed the injection system.

The set-up was a valve plus an intake duct and a plenum to model the 20 bar of injection pressure (Figure 6).

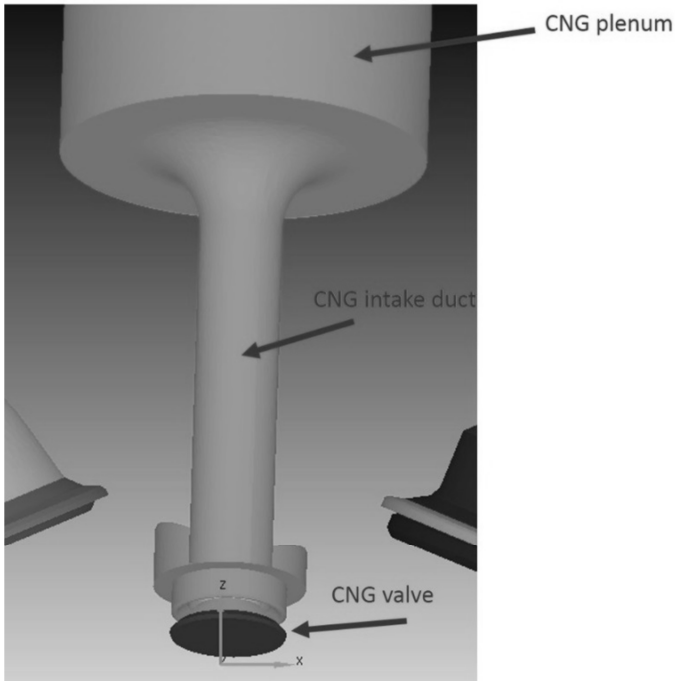

Figure 6: CNG valve model set-up

Thus the mixing was computed for different engine speeds considering the start of injection after the intake valve closing angle. The end of injection was determined to respect stoichiometric conditions in the combustion chamber (Table 2).

Table 2 : CNG injection set-up

Engine speeds (rpm)	Load conditions (Bar)	Start of injection (CAD from TDC)	End of injection (CAD from TDC)	In cylinder pressure at the end of injection (bar)
2000	3	-166	-162	0,5
2000	8	-166	-156	1
2000	Full	-166	-137	3,7
3000	8	-166	-150	1,2
5000	Full	-166	-90	6,9

In-cylinder pressure at the end of injection respected positive pressure loss versus the 20 bar at CNG inlet pressure and also the pressure limit allowed by the injector (11 bar).

During the experimental phase it was observed that the injection duration was between two and three time longer and led to higher in-cylinder pressure at the end of injection. This difference was attributed to lower pressure losses in the simulated simplified injector system compared to the real one and will be minimized by a new simulation work with the help of experimental data.

An homogeneity index was defined to determine the mixing quality, 1 corresponding to spatial perfect homogeneous mixing (Figure 7). Values were plot 20 crank angle before the TDC considering possible angle for spark ignition.

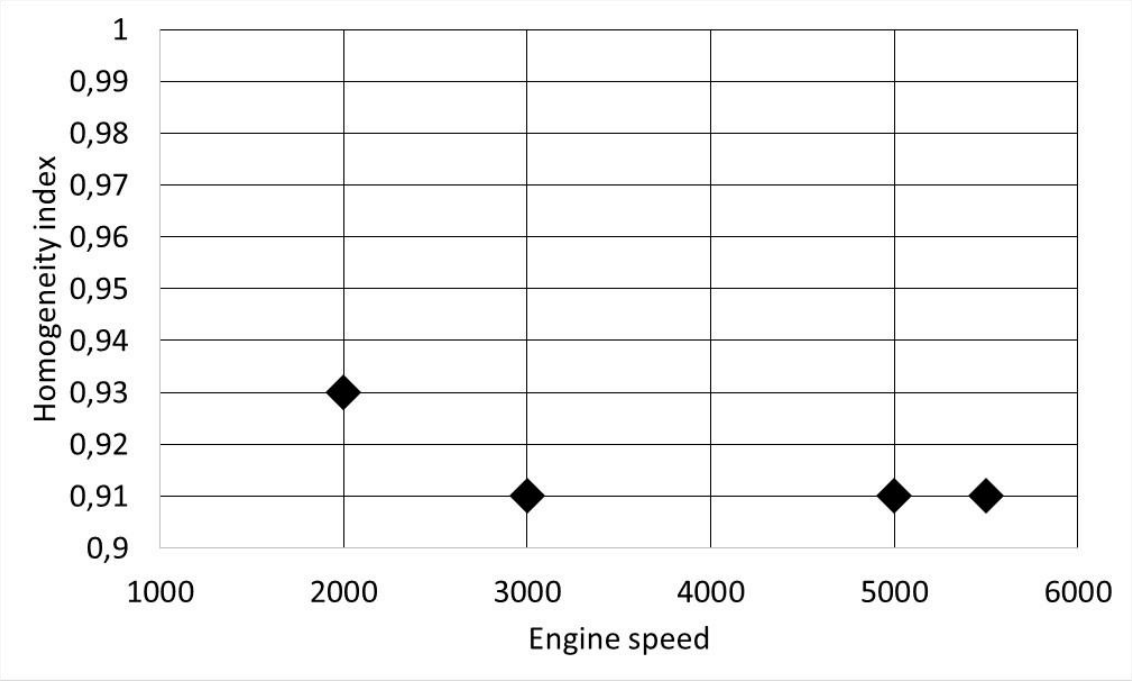

Figure 7: Homogeneity index versus engine speed (rpm) at 20 degree before TDC

As a conclusion, despite the differences in injection duration, the homogeneity index is considered satisfactory more especially at low engine speed. Over 3000 rpm, the engine speed has no impact on the mixing quality.

3 Experimental study

3.1 Engine specifications, measurements and procedure

The tests were carried out on a SI-SCE totally dedicated to CNG stoichiometric combustion with a 405 cm^3 displacement and a compression ratio of 13.4:1 (Table 1). The engine was based on a Renault 1.6L 4 valves Diesel engine with a variable valve timing (VVT) on both intake and exhaust camshafts. The single cylinder was equipped with a direct gas injection system. The cylinder head were designed according to the best results obtained from the modelling study. The intake and exhaust valve lift laws and timings were taken similar to previous study[6] for comparison. The piston had a central shallow bowl facing the injector and the spark plug. This design had proved its potential and remained similar to the one of the previous study[6].

Table 2: Single Cylinder Engine specifications

Engine displacement	405 cm^3
Bore / Stroke	80 mm / 80.5 mm
Compression ratio	13.4:1
Piston	Central shallow bowl
Ignition system	Mercedes Coil (90 mJ) NGK spark plug (ILZKR8A)
Intake valve	Opening duration = 169 CAD / maximum lift = 8.5 mm IVO = -6 ATDC / IVC = -5 ABDC
Exhaust valve	Opening duration = 200 CAD / maximum lift = 8.5 mm EVO = +38 BBDC / EVC = -18 BTDC
Fuel system	Continental CNG-DI prototype MFR = 12 g/s Maximum fuel pressure = 20 bar Maximum cylinder pressure = 11 bar
Engine limits	Average maximum cylinder pressure = 160 bar Average maximum cylinder pressure + 2σ = 180 bar Max air pressure = 3 bar Maximum exhaust temperature = 850°C

The direct injection system developed by Continental consisted in a moderate pressure prototype injector associated to its driving box. The injector was a solenoid type actuator and delivered an accurate and high flow rate of about 12 g/s. It operated at a fuel pressure of 20 bar and a maximum cylinder pressure of 11 bar allowing a latest End Of Injection (EOI) of about 64 CAD BTDC at full load. Gas consumption was measured by a MicroMotion CMF010 Coriolis type mass flow meter.

Turbocharged conditions were simulated with a set of chocked flows that allows regulation and measurement of the air flow. An air heater was implemented on the circuit to simulate the air temperature induced by the compressor and regulated by the air cooler. The exhaust backpressure was set using an exhaust throttle which was regulated in position, to match with the exhaust back pressure generated by all the restrictions along the actual MCE exhaust line (turbine, after treatment device, muffler,…).

LP-EGR conditions were simulated with a set of a valve, double compressors and exchangers that allowed the regulation of exhaust gas flow and temperature and their measurement.

In-cylinder pressure was monitored by a flush mounted cooled AVL QC34D pressure transducer. The pressure signal was acquired for every 0.1 CAD and the acquisition process covered 100 complete cycles. The average value of these cycles was used as pressure data for the calculation of combustion parameters. Engine-out exhaust gases (HC, CH_4, CO, CO_2, O_2, NOx) were analysed by an AVL AMA4000 analyser.

Tests at full load were performed at the targeted IMEP and engine differential pressure assessed to achieve the desired performance and to respect the engine mechanical and thermal limits.

Tests at part load were operated at the exhaust throttle position identical to the full load one for a selected engine speed.

An energy balance is calculated starting from the effective power adding all the estimated losses to come back to the initial introduced energy content. The different losses are evaluated such as pumping losses, exhaust losses, unburned fuel energy, wall heat exhaust losses (according to no adiabatic combustion analysis).

3.2 Fuel properties

Commercial grid CNG had very stable properties during this study (Table 2).

Moreover CNG properties did not vary significantly between the GasOn and Mogador[6] studies. For instance the lower heating value (LHV) difference did not exceed 1%. Therefore within this study, to compare the performance to current gasoline engine it was preferred to express the specific fuel consumption with regard to the gasoline energy content. Thus, the Indicated Specific Fuel Consumption was corrected with the gasoline LHV according to the following formula and is referred as ISFCc.

$$ISFCc = ISFC \cdot LHVgas / LHVgasoline$$

Table 3: Average CNG properties

Properties	CNG (average)
Lower heating Value (MJ/kg)	47.0 ± 2.1
Methane (% mass)	91.95 ± 0.55
Ethane (% mass)	4.54 ± 0.23
Propane (% mass)	0.59 ± 0.13
Nitrogen (% mass)	1.09 ± 0.13
H/C (mol/mol)	3.82 ± 0.01
Stoichiometric AFR (kg/kg)	16.1 ± 0.1
MON	126 ± 1

The purpose of this experimental test phase on a SCE was to validate the new combustion chamber design obtained by simulation. The improvement brought by this optimized design has been highlighted through the optimized injection timing, the global engine behaviour and the tolerance to EGR over the entire operating range.

3.3 Optimized injection timing

Direct injection (DI) brings several advantages. DI can be intended to improve the volumetric efficiency when using late injection i.e. after the Intake Valve Closure (IVC). Besides, DI phasing strategies can be used to improve air-fuel mixing applying early injection (to be closer to the PFI case) or to adopt later injection timing for solving scavenging issues or aftertreatment heating requirement. Only the mixing strategy was examined on this GasOn study as for Mogador study. For both studies, injection timing was therefore optimized to find the best trade-off between the good mixture homogeneity favoured at early injection and the high volumetric efficiency insured at late injection.

Thus, Start Of Injection (SOI) values were varied in a large range starting after the Exhaust Valve Closure (EVC = 378 CAD BTDC) at 340 CAD BTDC to a minimum given by the EOI limit (64 CAD BTDC), by step of 20 CAD around the IVC, for different loads and engine speeds, without EGR.

The volumetric efficiency was globally constant at early injection when SOI values were above 240 CAD BTDC then increased by almost 0.1 when the injection started just after the IVC (185 CAD BTDC) and remained at its maximal value for later injection timings (Figure 8).

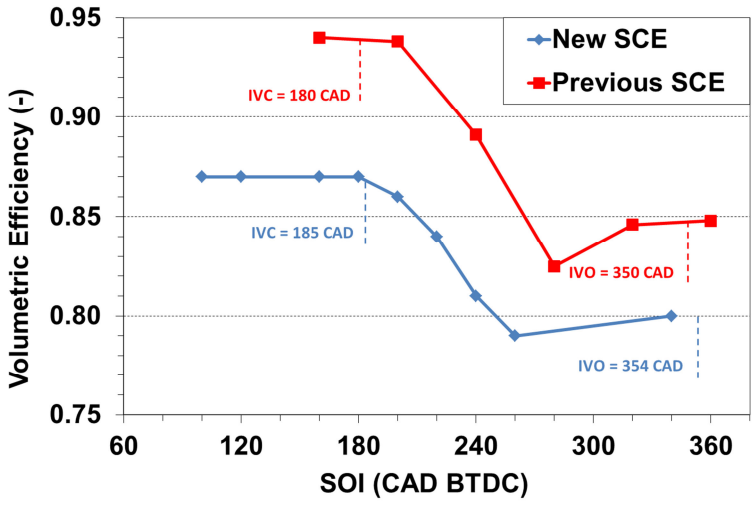

Figure 8: Volumetric efficiency as a function of SOI at 2000 rpm and IMEP of 15 bar

This trend was similar for different loads at 2000 rpm but also for other engine speeds and loads as well as for Mogador study[6] as shown on Figure 8 at the same load and speed using similar intake pressure. For both studies, the intake pressure evolved as expected, high in the early injection case and minimal for the late injection ones around the IVC. The volumetric efficiency was higher for the previous engine and is explained by the higher permeability (Figure 5).

The fuel consumption and combustion instability were low at early injection and became higher at late injection (Figure 10). The low fuel consumption and instability at early injection were associated to low HC emissions consequently to low unburned fuel energy losses (Figure 10). These results were mainly attributed to the high turbulence of the combustion chamber which favoured a good homogeneous mixture during the long time available before the ignition. The benefit of the high volumetric efficiency at late injection did not lead as expected to a reduction of the fuel consumption. This was due to the mixture heterogeneities caused by a lack of mixing time before spark and was corroborated by high combustion instabilities and higher intake pressure required to maintain the load.

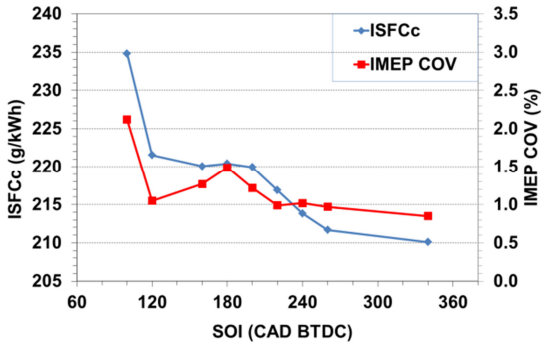

Figure 9: ISFC as a function of SOI at 2000 rpm and IMEP of 15 bar

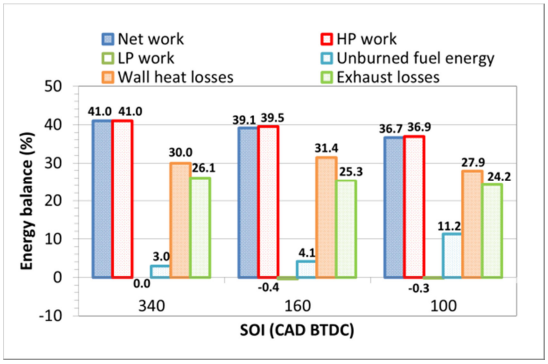

Figure 10: energy balance for various SOI at 2000 rpm and IMEP of 15 bar

Therefore, the benefit brought by the gain in volumetric efficiency with late injection was counterbalanced by a loss of combustion efficiency due to mixture heterogeneity. Consequently, the optimized engine efficiency appeared to be when the injection occurs during the intake stroke. The injection was therefore set at 340 CAD BTDC for engine speed above 2000 rpm and set at 260 CAD BTDC for the lower engine speed. To conclude on injection phasing, early injection will also help to reduce the injector gas pressure and thus will improve the vehicle range.

These results also showed that the DI injector can deliver an accurate gas mass flow rate (MFR from 8 to 64 mg/stroke) over the entire load range (IMEP from 3 to 30 bar) and especially a high gas MFR near full load.

It is thus demonstrated that DI is not beneficial for volumetric efficiency gain but leads to lowest fuel consumption at early injection by improving mixture homogeneity. It is reminded that DI remains attractive in order to optimize the injection phasing for instance during scavenging[4] or for aftertreatment[5] strategies as mentioned before. The interest regarding maximum load achievement might be highlighted with a real charging device on a MCE.

3.4 Global engine behaviour

This new SCE was compared to the previous single cylinder also totally dedicated to CNG[6] at low load (IMEP = 3 bar) and at high load (IMEP = 25 bar) for different engine speeds with similar intake pressure for both engines.

The fuel consumption and HC emissions were significantly lower for the new engine compared to the previous one (Figure 11 and Figure 12). The gas consumption gain was higher at low engine speed and was about 20 g/kWh at low load and 15 g/kWh at high load at 1500 rpm which represents a gain of about 7 %. The minimum consumption ISFCc at 2000 rpm and high load reached 209 g/kWh for the newly designed engine instead of 217 g/kWh for the previous one, that represents a gain of almost 4%. This improvement decreased with engine speed since fuel consumption gets closer when reaching 4500 rpm (gain ~1 %). Part of the gain came from lower HC emissions which were improved by less than 3 g/kWh at part load and less than 1 g/kWh at high load. These slight reduced emissions were related to earlier injection favouring a better homogeneity of the mixture.

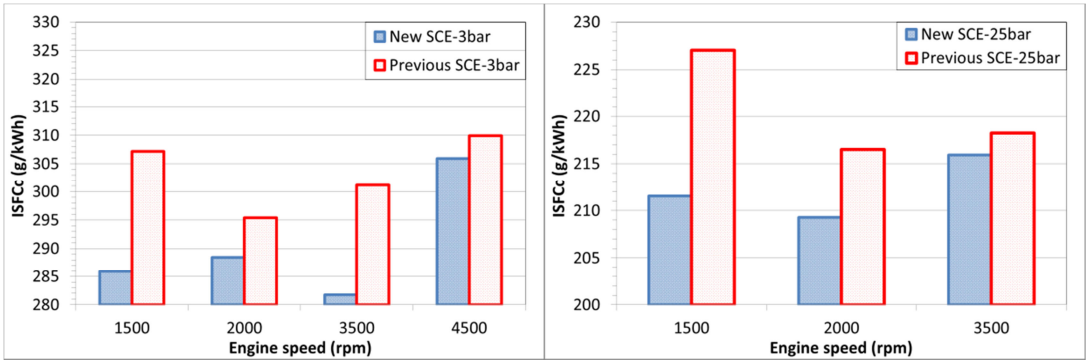

Figure 11: ISFCc as a function of engine speed for new and previous engines at IMEP of 3 bar (left) and 25 bar (right)

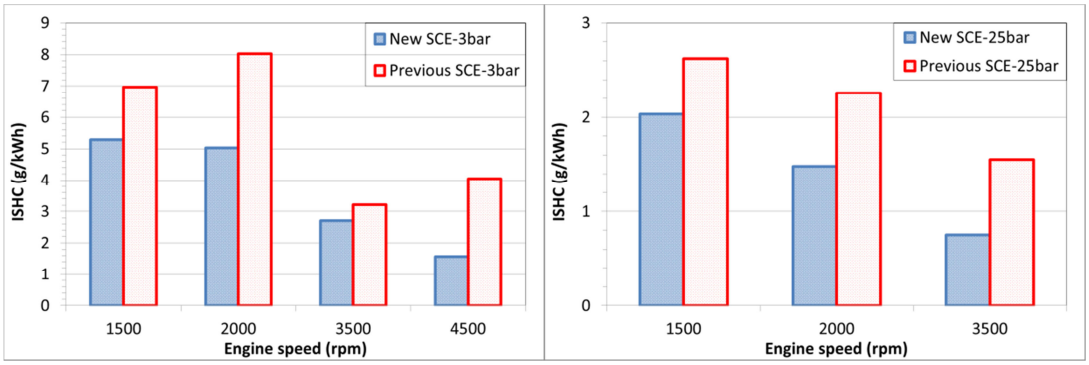

Figure 12: ISHC as a function of engine speed for new and previous engines at IMEP of 3 bar (left) and 25 bar (right)

Another explanation comes from the better combustion efficiency shown by a higher maximum Rate of Heat Release (Max ROHR) for the new engine compared to the previous one (Figure 13 and Figure 14). This new design favours fast combustion at low engine speeds but affects it at high engine speeds and loads. This higher combustion rate corroborates the high turbulence simulated and measured on the new cylinder head design. The combustion rate evolution as a function of engine speed is also well correlated to the simulated homogeneity index (Figure 7).

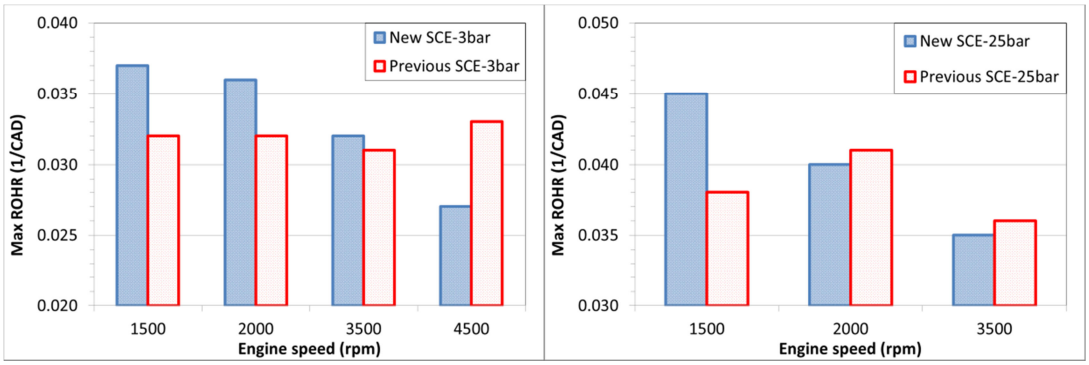

Figure 13: Maximum ROHR as a function of engine speed for new and previous engines at IMEP of 3 bar (left) and 25 bar (right)

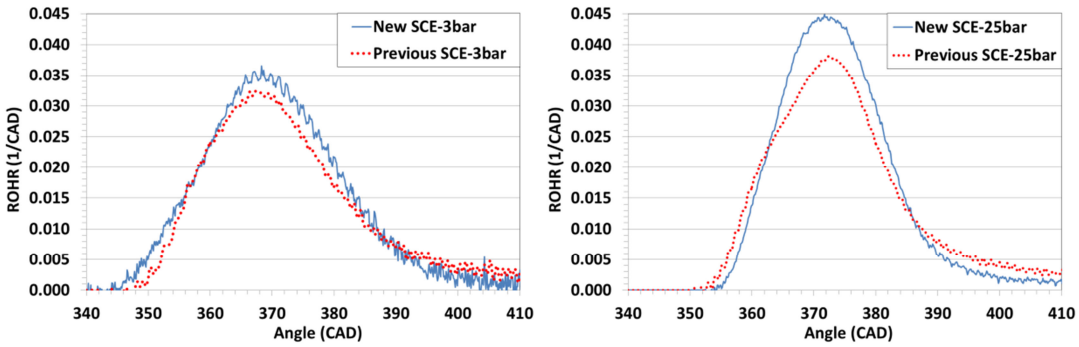

Figure 14: ROHR for new and previous engines at 1500 rpm at IMEP of 3 bar (left) and 25 bar (right)

The last explanations were brought by the energy balance calculation (Figure 15). These results confirmed the lower unburned losses for new engine especially at low load which could be attributed to the better homogenization brought by the higher turbulence in the chamber. The calculation also revealed the lower wall heat losses for the new engine which was ascribed to the higher combustion rate.

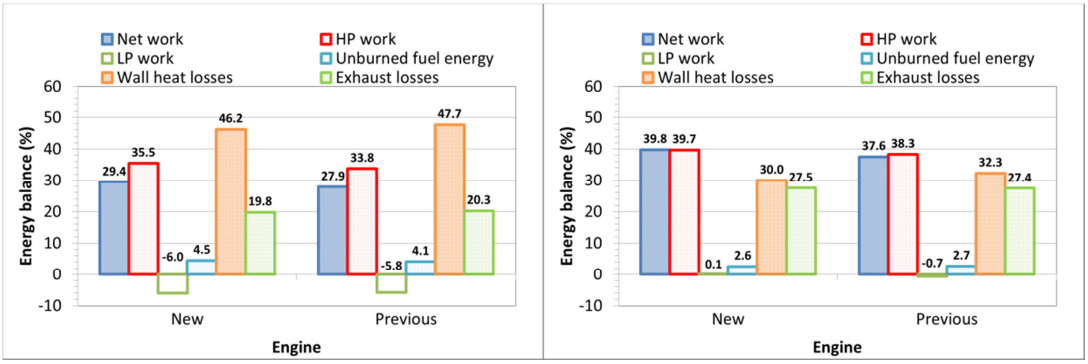

Figure 15: Energy balance for new and previous engines at 1500 rpm at IMEP of 3 bar (left) and 25 bar (right)

It is thus showed that new high-turbulence engine design insures a higher combustion rate at low engine speed which in turn allows a lower fuel consumption due to lower unburned fuel losses and wall heat losses.

This new performance was then verified on the EGR tolerance level at low engine speed and load for the new SCE.

3.5 Tolerance to EGR and corresponding performance improvement

LP-EGR tests were performed at low engine speed and low load to validate the higher dilution tolerance that the new-high turbulence engine design should brought and to allow reducing the pumping losses.

Besides, LP-EGR was also applied at high engine speed and high load to mitigate knock and to reduce the exhaust temperature.

For high engine speed tests performed at full load, the EGR rate was operated at 5 and 10 %, at engine speed above 2750 rpm, at the air pressure target. For the low engine and low load tests carried out at 2000 rpm and at IMEP of 4.6 bar, the EGR rate was increased up to a maximum close to 25 % by incremental steps of 5 %. In these conditions, the IMEP was maintained with LP-EGR but the intake air pressure has been increased by 0.3 bar. This extra level of pressure will definitely impact the technical definition and design of the turbocharger on the future MCE.

LP-EGR at high engine speed and full load

On the SCE at full load and high engine speed, the exhaust temperature did not exceed the tolerated limit without EGR (850°C) but EGR could be required for the turbine protection on MCE since exhaust temperature would be higher than for SCE due to a higher number of combustion per cycle. In these conditions the exhaust temperature was typically decreased with LP-EGR with a temperature drop of about 40°C for 10% of EGR rate (Figure 16) and an acceptable increased instability (Figure 17). This temperature drop was achieved by the higher spark timing (up to 5 CAD) allowed by the decrease of knock sensibility and intake gas mixture capacity brought by EGR. This gain could in turn be used to increase the output power up to the thermal limit. However it did not permit in this case to gain in fuel consumption as explained hereafter.

The combustion angular durations were also typically increased with EGR (Figure 18) that affects the local equivalence ratio and the in-cylinder temperature. The combustion was slowed down (Figure 19) which in turns slightly increased exhaust losses (Figure 20) and thus limited the gain in fuel consumption.

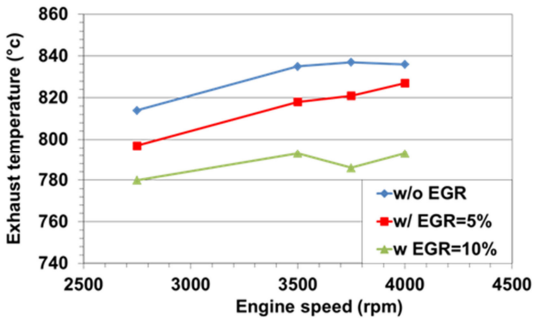

Figure 16: Exhaust temperature as a function of high engine speed at full load with LP-EGR at various rates

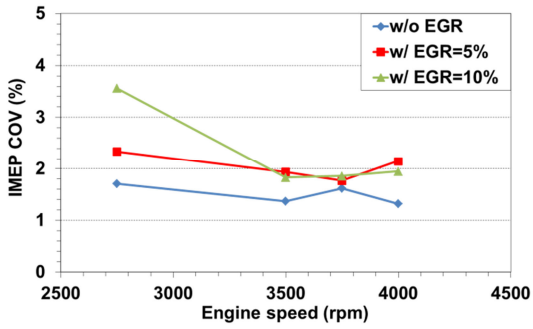

Figure 17: IMEP-COV as a function of high engine speed at full load with LP-EGR at various rates

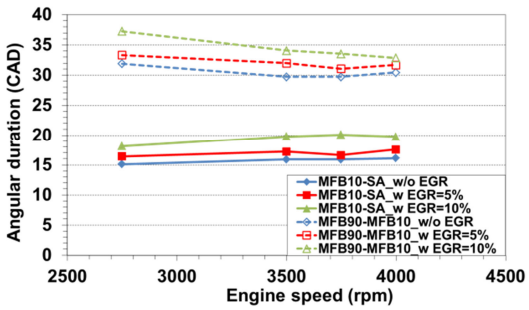

Figure 18: Angular duration as a function of high engine speed at full load and various EGR rates

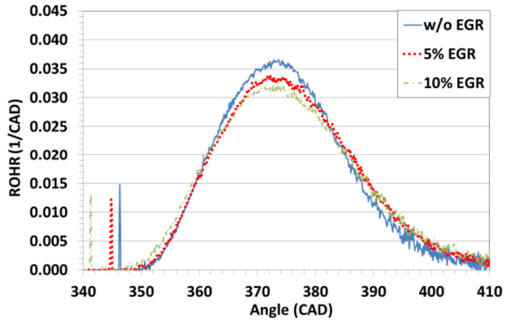

Figure 19: ROHR at 3500 rpm, full load and various EGR rates

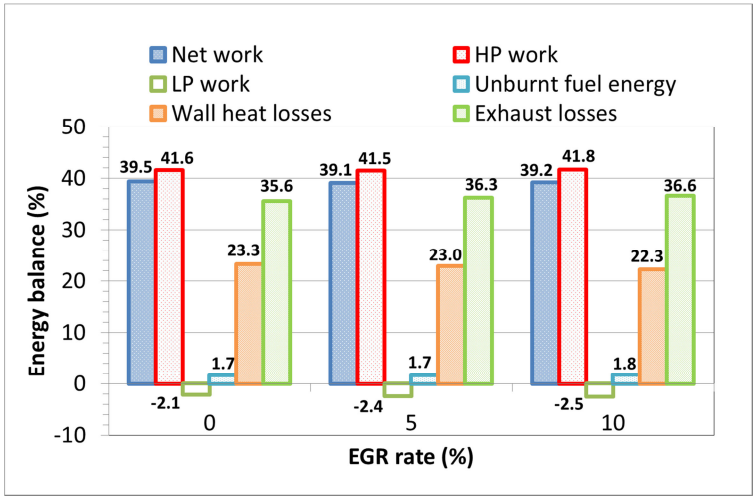

Figure 20: Energy balance for various EGR rate at full load and 3500 rpm

LP-EGR at low engine speed and part load

In these conditions, the increase of EGR rate typically favoured combustion instability leading to higher HC emissions (Figure 21 and Figure 22). At part load at 4.6 bar of IMEP, the engine tolerated a high level of EGR, close to 20 % (IMEP COV below 5 %) associated to an extra HC of 3 g/kWh.

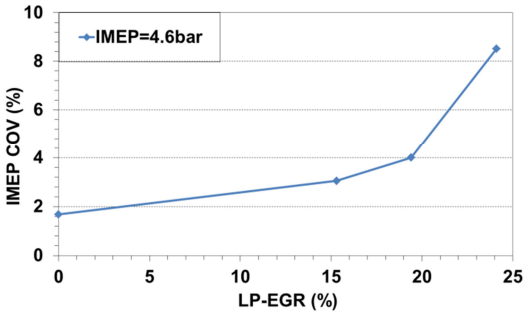

Figure 21: IMEP COV as a function of EGR rate at 2000 rpm and 4.6 bar

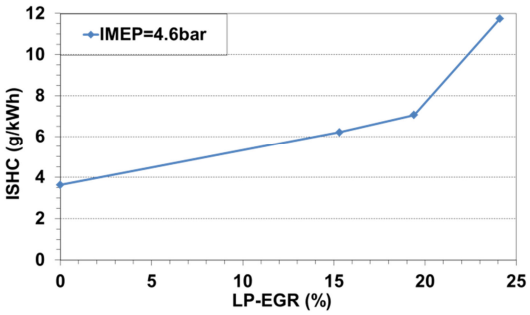

Figure 22: ISHC as a function of EGR rate at 2000 rpm and 4.6 bar

The combustion rate typically decreased with EGR rate up to the limit by affecting the local equivalence ratio (Figure 24). The EGR rate limit was very high, reaching a value close to 20 %, which was due to the high combustion rate induced by the high turbulence cylinder head design.

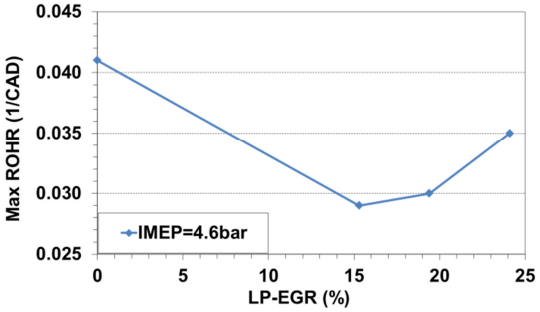

Figure 23: Max ROHR as a function of EGR rate at 2000 rpm and 4.6 bar

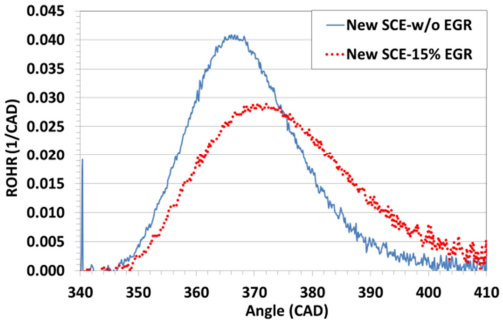

Figure 24: ROHR (right) at 2000 rpm and 4.6 bar without and with EGR

Moreover, fuel consumption was improved when EGR rate was close to the EGR tolerance limit (Figure 25). The maximum fuel consumption drop was about 2 g/kWh at 4.6 bar and 15 % EGR (consumption gain close to 1 %).

This gain was attributed to the lower pumping losses as well as the lower wall heat losses at low load as shown on Figure 26 and despite the slightly higher unburned and exhaust losses.

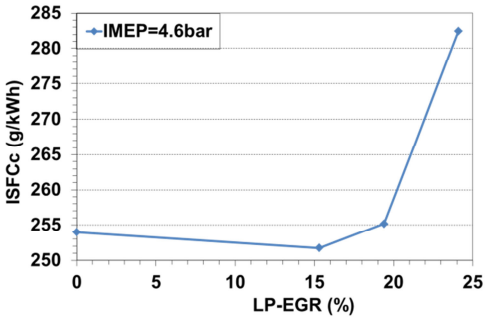

Figure 25: ISFCc (left) and LP-IMEP (right) as a function of EGR rate at 2000 rpm and 4.6 bar

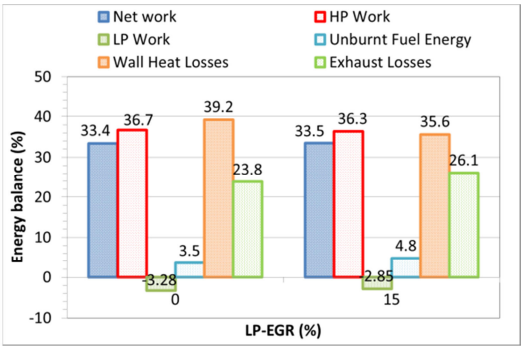

Figure 26: Energy balance at 2000 rpm and 4.6 bar without and with EGR

These results confirmed the positive effect of the LP-EGR allowing to mitigate knock and to reduce exhaust temperature at high engine speeds and loads allowing to increase the output power in these conditions. Moreover, EGR allowed improving the engine indicated efficiency (up to 2 %) by lowering pumping losses and wall heat losses at low load up to high rate limit allowed by the newly high turbulence cylinder head design.

3.6 Overview of the new engine design performance

The final statement of the performance achieved with this newly designed gas combustion engine is gathered into the map showed below.

The full load curve of the new engine showed a maximum IMEP close to 31 bar (Figure 27 and Figure 28) over a large range of engine speed (1500 to 3000 rpm). In these conditions, the targeted performance was easily achieved below 2750 rpm since the hardware resistance criteria (maximum cylinder pressure) were not reached. The limit comes from the boost pressure (P2 = 3bar). The engine power output could also be improved by scavenging the combustion chamber with a positive valve overlap[6] at low engine speed but it was not done in these tests. At high engine speed, above 2750 rpm, the performance was close to the cylinder pressure and temperature limits due to knock appearance despite the high octane equivalent number of CNG. This could be explained by the high exhaust pressure causing a significant increase of the rate of residual burned gases in the combustion chamber. It could also be related to the cylinder head design made to sustain high in cylinder pressure involving important wall deck thickness that can affect the heat exchange capacity. The knock occurrence can be mitigated by using LP-EGR as shown previously.

The ISFCc map showed the lower fuel consumption for this new highly turbulent gas engine compared to the previous one[6] with a large zone of lower value around the mid-engine speed and high-load, which was respectively below 210 g/kWh and 220 g/kWh (Figure 27). This good result can also be illustrated through the indicated efficiency. The highest value is above 41% for the new engine over a large operating range which represents a 2 point efficiency improvement in comparison to the previous engine[6] (39%) (Figure 28). This high indicated efficiency is close to the value attained on Diesel engine and is thus very interesting.

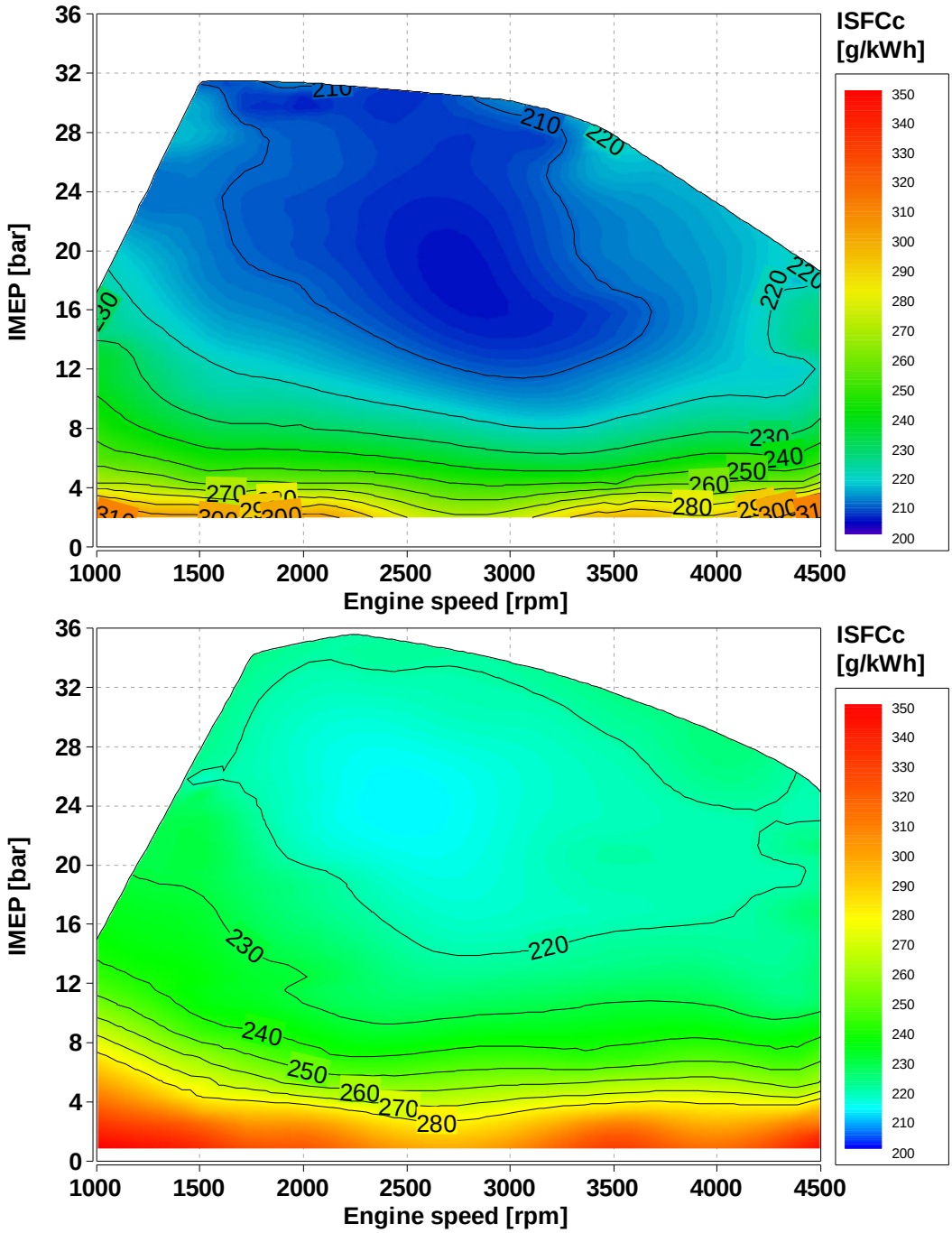

Figure 27: ISFCc maps for new engine (up) and previous engine (down)

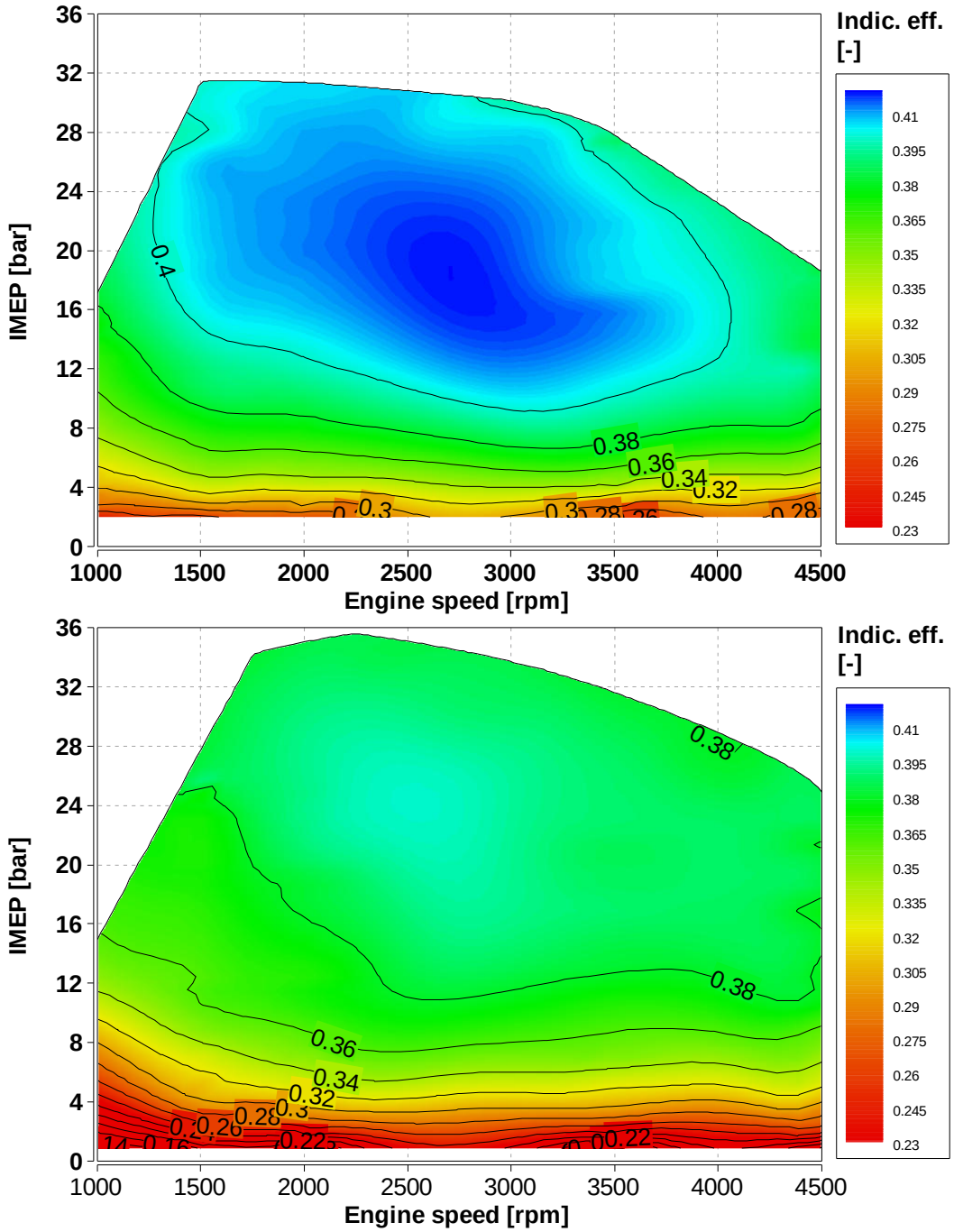

Figure 28: Indicated efficiency maps for new engine (up) and previous engine (down)

4 Summary and conclusions

A new CNG-DI cylinder head was designed within the H2020 GasOn European project. The purpose was to increase the turbulence of the high compression ratio gas SI engine based on Diesel core and running in homogenous stoichiometric conditions in order to improve the combustion process and to exploit all the CNG properties.

The new cylinder head was designed by 3D simulation to increase the turbulence in the combustion chamber without altering too much the permeability compared to a previous study. Flow bench results on a manufactured cylinder head confirmed the higher level of turbulence compared to the previous one with a moderate decrease in flow capacity.

This manufactured cylinder head was then mounted on a SCE based on Renault Diesel engine equipped with a high mass flow rate CNG-DI injector prototype developed by Continental within the GasOn project.

The CNG-DI led as expected to higher volumetric efficiency at late injection but the gas consumption was affected in this case by higher unburned losses due to a lack of mixture homogeneity. The indicated efficiency was thus optimal at early injection allowing to insure a good mixture homogeneity and to decrease CNG pressure, then improving the vehicle range. The results also confirmed the accurate and high flow rate of direct gas injector at every load. Moreover, DI could be used in optimized injection phasing for scavenging and aftertreatment strategies.

Besides, the new cylinder head design led as expected to higher combustion velocity, especially at low engine speed compared to the previous engine. It thus allowed to achieve the targeted performance (~240 N.m/L at 1500 rpm, ~80kW/L at 4500 rpm) and gain in indicated efficiency (41 % against 39 %) due to lower unburned losses and wall heat losses.

The optimized cylinder head configuration also allowed to favour LP-EGR tolerance up to a high rate (20 %) at low engine speed and load. Besides, EGR permitted to gain 2% in indicated efficiency in these conditions due to lower pumping losses. It also allowed to mitigate knock and to reduce the exhaust temperature at high engine speed and full load and therefore to increase the output power up to the thermal limit. However, EGR required an extra boosting pressure and thus a larger and most expensive turbocharger.

The next steps of the project will validate this combustion system on a multicylinder and optimize the engine key parameters such as air-fuel mixture in respect with the injection pattern, the optimization of the air path system, valve timing and lift to assess the capability of a dedicated gas engine to compete with a Diesel engine.

5 Acknowledgments

The authors would like to acknowledge the support of GasOn H2020 European Project for this work.

The authors would also like to thank Geoffrey Bourrachot and Jocelyn Terver, technicians at IFPEN for the test bench work as well as Matthieu Lecompte for the fruitful discussions.

6 Definitions/Abbreviations

AFR: Air/Fuel Ratio

ATDC, BTDC, TDC: After Top Dead Centre, Before Top Dead Centre, Top dead centre

ABDC, BBDC, BDC: After Bottom Dead Centre, Before Bottom Dead centre, Bottom dead Centre

CAD: Crank Angle Degree

CFD: Computational Fluid Dynamic

CNG: Compressed Natural Gas

CR: Compression Ratio

DI: Direct Injection

EGR, LP-EGR: Exhaust Gas Recirculation, Low pressure Exhaust Gas Recirculation

EOI: End Of Injection

EVC: Exhaust Valve Closing

EVO: Exhaust Valve Opening

HC: Hydrocarbon content

ICE: Internal Combustion Engine

IMEP, LP-IMEP, IMEP COV: Indicated Mean Effective Pressure, Low Pressure Indicated Mean Effective Pressure, Indicated Mean Effective Pressure Coefficient Of Variation

Indic. Eff.: Indicated Efficiency

ISFC, ISFCc: Indicated Specific Fuel Consumption, corrected Indicated Specific Fuel Consumption: ISFCc = ISFC LHVgas / LHVgasoline

ISHC: Indicated Specific HC (hydrocarbons)

IVC: Inlet Valve Closing

IVO: Inlet Valve Opening

LD: Light Duty

LHV: Low Heating Value of CNG

LHV, LHVgasoline: Low Heating value of CNG, Low Heating Value of gasoline

MAF: Mass Air Flow Rate

MFR: Gas Mass Flow Rate

ROHR, Max ROHR: Rate of Heat Release, maximum Rate of Heat Release

MCE: Multi-Cylinder Engine

MN: Methane Number

MON: Motor Octane Number

RANS model: Reynold Average Navier-Stokes equations

RNG model: Re-Normalisation Group methods to renormalize the Navier-Stokes equations

RON: Research Octane Number

N: engine speed

PC: Passenger Car

SCE: Single Cylinder Engine

SI: Spark Ignition

SOI: Start Of Injection

Vol. Eff.: Volumetric Efficiency

VVT: Variable Valve Timing

7 Reference List

[1] Woldwide emissions standards – Passenger cars and light duty vehicles, Delphi, 2016-2017, http://delphi.com/docs/default-source/worldwide-emissions-standards/delphi-worldwide-emissions-standards-passenger-cars-light-duty-2016-7.pdf

[2] EUROSTAT, European commission, Passenger cars in EU, http://ec.europa.eu/eurostat/statistics-explained/index.php/Passenger_cars_in_the_EU, April 2017.

[3] S. Taniguchi, Y. Tsukasaki and A. Yasuda, "Study of compressed natural gas direct injection engine", FISITA paper No. F2006P089, (2006).

[4] J.F. Preuhs, G. Hofmann, J. Kirwan, Natural gas injection for Low CO2 spark Ignition engine SAE SIA 2015.

[5] P. Hofmann, T. Hofherr, G. Hoffmann, J.F. Preuhs, Potentual of CNG Direct Injection for Downsizing Engines, MTZ 07-081-2016.

[6] B. Douailler, F. Ravet, V. Delpech, D. Soleri, B. Reveille, R. Kumar, Direct Injection of CNG on High Compression Ratio Spark Ignition Engine: Numerical and Experimental Investigation, SAE International 2011-01-0923.

[7] M. C. Haeng, H. Bang-Quan, Spark Ignition natural gas engines – a review, Energy Conversion and Management 48 (2007) 608-618.

[8] D. Seboldt, D. Lejsek, M. Wentsch, M. Chiodi, M. Bargende, Numerical and Experimental Study on Mixture Formation with a Outward-Opening Nozzle in a SI Engine with CNG-DI, SAE International 2016-01-0801.

[9] Converge Science, https://convergecfd.com/.

[10] Yakhot, V., Orszag, S.A., Thangam, S., Gatski, T.B. & Speziale, C.G., Development of turbulence models for shear flows by a double expansion technique, Physics of Fluids A, Vol. 4, No. 7, pp1510-1520 (1992).

[11] N. Peters, Turbulent combustion, Cambridge Press, 2000.

[12] C. Mounaïm-Rousselle, L. Landry, F. Halter, F. Foucher, Experimental characteristics of turbulent premixed flame in a boosted spark ignition engine, Proceedings of the Combustion Institute 34 (2013) 2941–294.